

Experimental Study of Overturning Prevention for Lunar and Planetary Lander by Optimizing Footpad Tilt Angle

Kentaro Matsuura (The University of Tokyo), Takao Maeda (Chuo University) and Tatsuaki Hashimoto (JAXA)

Abstract

In future lunar and planetary exploration, landing missions in scientifically interesting regions will be conducted. However, such areas have a rough surface and are difficult to touch down safely. The previous study implies that by designing the tilt angle of the footpad, which is the only part in contact with the surface of the celestial body, it is possible to prevent overturning even when the lander touches down with horizontal speed. In this study, we conduct a landing experiment using footpads with different tilt angle and analyze the difference of landing behavior concerning footpad tilt angle.

月惑星着陸機のフットパッド取り付け角度最適化による耐転倒性向上に向けた実験的検討

松浦賢太郎（東京大学），前田孝雄（中央大学），橋本樹明（宇宙航空研究開発機構）

摘要

将来の月惑星探査では、科学的に調査価値が高いものの従来は着陸が困難であった不整地への着陸が求められている。従来の検討により、着陸機において唯一天体表面と接触する部位であるフットパッドの取り付け角度を適切に設計することで、水平方向速度を持って着陸する場合であっても転倒を防止できる可能性が示されている。本研究では、着陸機モデルを用いた落下試験により、フットパッドの取り付け角度が着陸時の姿勢変動に与える影響を検討する。

1. Introduction

Future lunar and planetary exploration missions require landing in rough areas where conventional landers could not reach. To achieve safe touch down on such areas, a landing gear with functions to prevent overturning is necessary.

The simplest approach for overturning prevention is to expand the width between the legs of the lander. For example, the Apollo landing module was equipped with a deployment mechanism for the landing gear [1]. A landing gear system based on a moment exchange impact lander [2] and an attitude control method based on a variable-damping shock absorber were proposed. However, previous methods are unsuitable for small landers whose payload is limited and the width between the legs is not enough to install complex mechanisms.

Footpad is the only part that contacts the surface of the celestial body. The force exerted on the lander body depends on the force acts on the footpads. In the Apollo project, many experiments were conducted to analyze

the interaction force between the footpad and the terrain. In addition, the relationship between the footpad tilt angle and the drag force [3] was studied and the impact force and the penetration sinkage of different types of footpads were measured [4]. The results of the previous studies show that shape and tilt angle have a significant effect on the force acts on the footpad.

In this paper, we describe a footpad tilt angle design method for overturning prevention of a lunar and planetary lander. Section 2 reviews the interaction force estimation method based on RFT. Section 3 describes the relationship between the footpad tilt angle and the overturning prevention effect. Sections 4 and 5 validate the effectiveness of the proposed footpad tilt angle design method by simulation and experiment respectively. Section 6 shows the summary and future work.

2. Footpad-Soil Interaction Model

The surface of the Moon and rocky planets is covered with fine and loose sand called regolith. In order to

analyze the dynamics of the lander, it is important to estimate the interaction force against the soil. Many types of interaction models have been studied in the field of terramechanics, which was originated by M.G. Bekker. However, it is difficult to apply the prior terramechanics models to estimate the force acting on the footpad of a lander that dynamically penetrates the soil.

In this research, we use Resistive Force Theory (RFT) [6] to estimate the interaction force. RFT is a semi empirical method proposed by Li et al. In RFT, the force acting on an element which traverses in the granular media is obtained by the following equation,

$$F_{\{x,y\}} = \int_S \zeta \alpha_{\{x,y\}}(\beta, \gamma) |d| dS \quad (1)$$

where, S is the leading surface of the mechanical part that traverses the granular media, α_x and α_y are the vertical and horizontal generalized stresses per unit depth d , and ζ is a scaling factor, which represents the characteristics of the soil. The stress function depends on the attack angle β and the penetration angle γ . $A_{m,n}$, $B_{m,n}$, $C_{m,n}$, $D_{m,n}$ are the coefficients obtained by experiments. The values are listed in Table 1.

$$\alpha_y(\beta, \gamma) = \sum_{m=-1}^1 \sum_{n=0}^1 \left[A_{m,n} \cos 2\pi \left(\frac{m\beta}{\pi} + \frac{n\gamma}{2\pi} \right) + B_{m,n} \sin 2\pi \left(\frac{m\beta}{\pi} + \frac{n\gamma}{2\pi} \right) \right] \quad (2)$$

$$\alpha_x(\beta, \gamma) = \sum_{m=-1}^1 \sum_{n=0}^1 \left[C_{m,n} \cos 2\pi \left(\frac{m\beta}{\pi} + \frac{n\gamma}{2\pi} \right) + D_{m,n} \sin 2\pi \left(\frac{m\beta}{\pi} + \frac{n\gamma}{2\pi} \right) \right] \quad (3)$$

3. Footpad Configuration for Overturning Prevention

In this section, the footpad tilt angle design method for overturning prevention is described. We assume that the motion of the lander is limited to the x-y plane as shown in Fig. 3. When the lander touches down while it still possesses a horizontal velocity component, the inertia force generates overturning moment. To prevent overturning, the torque against the overturning should be maximized.

Assuming that the footpad is rectangular and flat, the force acts on the footpad is simplified as below:

Table 1 RFT parameters [6]

$A_{m,n}$	$n=0$	$n=1$	$B_{m,n}$	$n=0$	$n=1$
$m=-1$	0.000	0.000	$m=-1$	0.000	0.055
$m=0$	0.206	0.000	$m=0$	0.000	0.358
$m=1$	0.169	0.000	$m=1$	0.000	0.212
$C_{m,n}$	$n=0$	$n=1$	$D_{m,n}$	$n=0$	$n=1$
$m=-1$	0.000	0.007	$m=-1$	0.000	0.000
$m=0$	0.000	0.253	$m=0$	0.000	0.000
$m=1$	0.000	-0.124	$m=1$	0.088	0.000

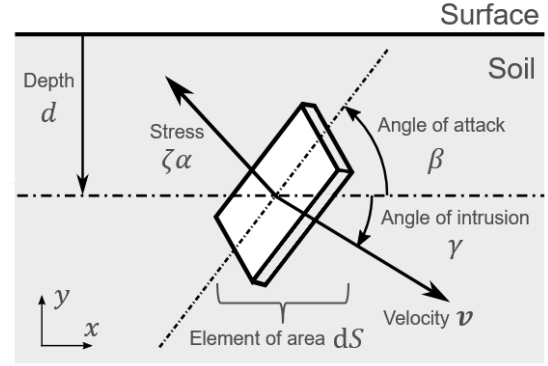


Figure 1 RFT model.

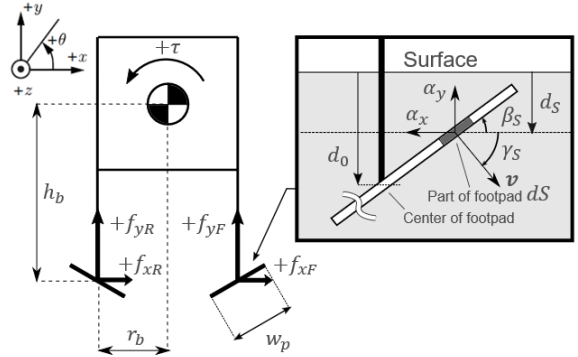


Figure 2 2D model of four legged lander.

$$f_{\{x,y\}} = r_p w_p d_0 \zeta \alpha_{\{x,y\}}(\beta, \gamma) \quad (4)$$

where r_p and w_p are the width of the footpad in x, y direction, respectively, d_0 is the depth of the center of the footpad, β is the angle of the footpad, γ is the penetration angle of the footpad. The torque exerted on the lander body by the footpads is

$$\tau = r_b f_{yF} + h_b f_{xF} - r_b f_{yR} + h_b f_{xR} \quad (5)$$

where r_b is equal to half of the width between the lander's legs, h_b is the height of the center of the gravity. f_{xF} , f_{yF} and f_{xR} , f_{yR} are the forces acts on the front and rear footpads, respectively. Eq. (5) can be expressed by using an aspect ratio $A_R = h_b/r_b$ and the pressure function $\alpha_{x,y}(\beta, \gamma)$ as below:

$$\tau = r_p w_p d_0 r_b \zeta \{ \alpha_y(\beta_F, \gamma) - A_R \alpha_x(\beta_F, \gamma) - \alpha_y(\beta_R, \gamma), -A_R \alpha_x(\beta_R, \gamma) \} \quad (6)$$

Eq. (6) depends on the front and rear footpad angle β_F and β_R and the penetration angle γ . To prevent overturning, the torque should be maximized. Therefore, we can design the angle of the footpad by seeking the angle which maximizes the torque.

Examples of the configurations of footpad tilt angle are shown in Fig. 4. In previously published work, it was assumed that the front and rear footpads were mounted to the landing legs symmetrically [7]. For the symmetrical configuration, the optimal angle can be obtained analytically and based only on the aspect ratio of the lander; besides, the overturning prevention effect is valid regardless of the landing direction.

On the other hand, the asymmetry configuration can obtain higher torque than the symmetry configuration. As an example, the relationship between the footpad angles β_F and β_R and the torque acting on the lander τ where the aspect ratio $A_R = 2$, the horizontal speed $v_x = 2$ m/s, the vertical speed $v_y = -3$ m/s. The optimal angles which maximize the torque are $\beta_R = -56.7^\circ$ and $\beta_F = -14.4^\circ$.

Fig. 6 shows the relationship between the torque τ and the penetration angle γ where $\beta_R = -56.7^\circ$ and $\beta_F = -14.4^\circ$. In the case $v_x = 2$ m/s and $v_y = -3$ m/s, the torque of the asymmetry configuration is positive (against overturning direction). The torque of the symmetry and nominal configuration are both negative (overturning direction), though the symmetry configuration suppresses the overturning torque. According to the preceding results, the asymmetry configuration possesses a more effective overturning prevention effect than the symmetry configuration. Here, note that the optimal angle for the asymmetry configuration depends on not only the aspect ratio of the lander but also the penetration angle.

4. 2D Landing Dynamics Simulation

In this section, the overturning prevention effect of the proposed footpad configurations are verified with a dynamic simulation by MATLAB 2018b. The model used in the simulation is a small lunar lander whose size is almost same as SLIM, which was proposed by Japan Aerospace Exploration Agency [8]. The configurations of the footpad and the parameters of the simulation model are shown in Table 2 and 3, respectively. The condition of the simulation is shown

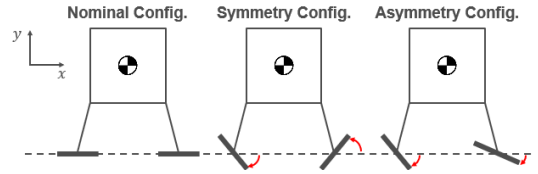


Figure 5 Examples of footpad configurations.

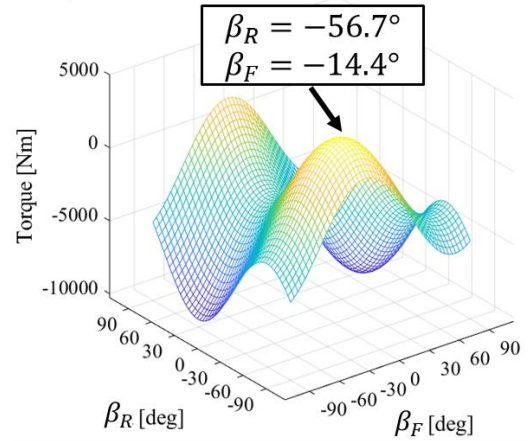


Figure 3 Relationship between the footpad angle and the torque.

$$(A_R = 2, v_x = 2 \text{ m/s}, v_y = -3 \text{ m/s})$$

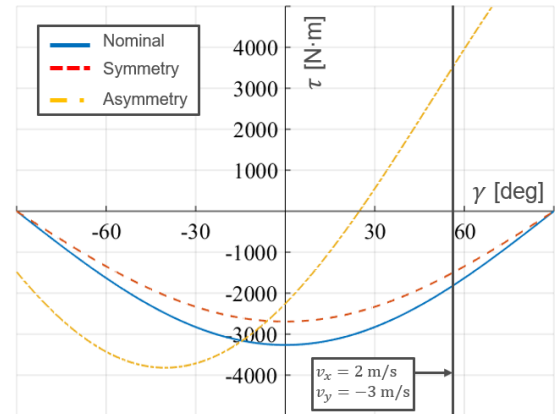


Figure 4 Relationship between the torque and the penetration angle.

$$(A_R = 2, \beta_R = -56.7^\circ, \beta_F = -14.4^\circ)$$

in Table 4. We assume that the lander will touch down on a flat surface covered with regolith and the gravitational acceleration is equal to that on the surface of the Moon.

Figure 7 shows example images of landing for the nominal, symmetry and asymmetry configuration, respectively. As for the asymmetry configuration, the lander touches down without overturning, though the nominal and symmetry configuration cause overturning. Compared with the nominal configuration, the symmetry configuration suppresses the inclination of the lander body.

Figure 8 shows the time histories of the force acting on the front and rear footpads. As for the symmetry configuration, the y directional force on the front footpad f_{yF} increases and it generates torque which prevents overturning. As for the asymmetry configuration, the horizontal force f_{xF} the angle of the front footpad is close to the penetration angle,

The results of the simulation show that the asymmetrical configuration is the most effective when the lander touches down towards $+x$ direction. However, it is assumed that the overturning prevention effect will deteriorate when the lander touches down $-x$ direction due to its asymmetry. To examine the stability for reverse landing, we analyzed the relationship between vertical velocity and acceptable horizontal velocity. Figure 9 shows the result. When the lander touches down with positive horizontal velocity, the acceptable horizontal velocity is getting higher in the order of nominal, symmetry, asymmetry. On the other hand, in the case that the lander touches down with negative horizontal velocity, the acceptable

horizontal velocity for the asymmetry configuration is higher than the other configurations when $|v_y| < 1.2$ m/s.

Table 2 Configurations of the footpads.

Configuration	Tilt Angle β_R	Tilt Angle β_F
Nominal	0 deg	0 deg
Symmetry	-18 deg	18 deg
Asymmetry	-57.6 deg	-14.4 deg

Table 3 Parameters of the lander.

Variable	Parameter	Value
m	Mass of lander	150 kg
J	Moment of inertia of lander	50 kg · m ²
h_b	Height of center of gravity	1.5 m
r_b	Radius of lander	0.75 m
r_p	Width of footpad (z axis)	2 × 200 mm
w_p	Width of footpad (x axis)	200 mm

Table 4 Simulation condition.

Variable	Parameter	Value
g	Gravity acceleration	1.62 m/s ²
ζ	Scaling factor of terrain	1.0
$y(0)$	Initial height of COG	$h_b + 0.1$
v_x	Horizontal velocity	2 m/s
v_y	Vertical velocity	-3 m/s

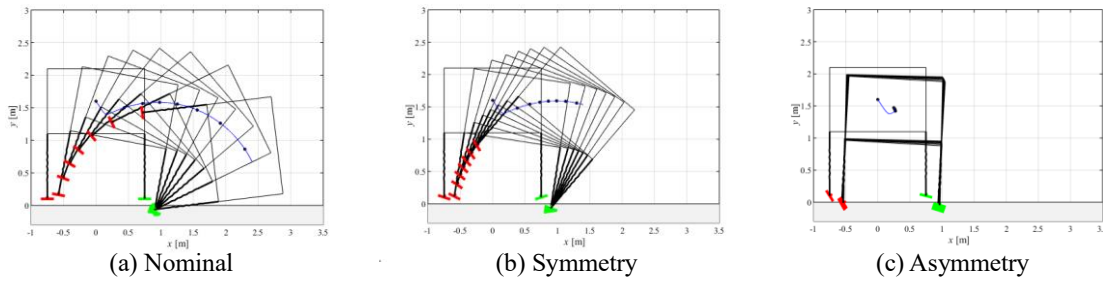


Figure 7 Example images of landing ($t = 0 \sim 3$ sec)

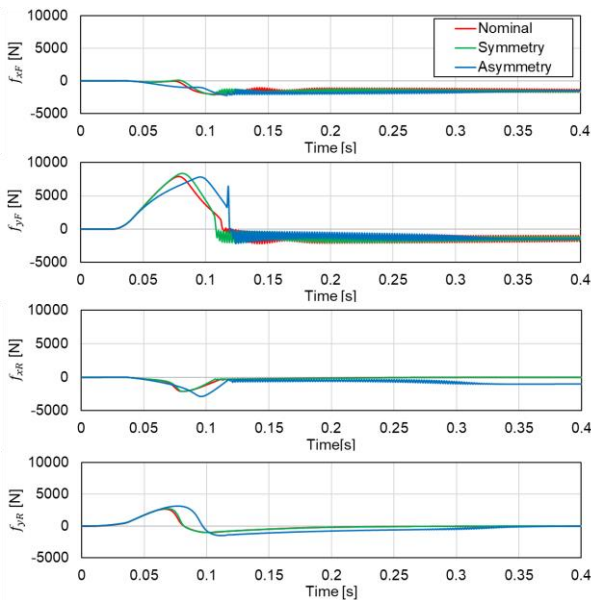


Figure 8 History of force on the footpads

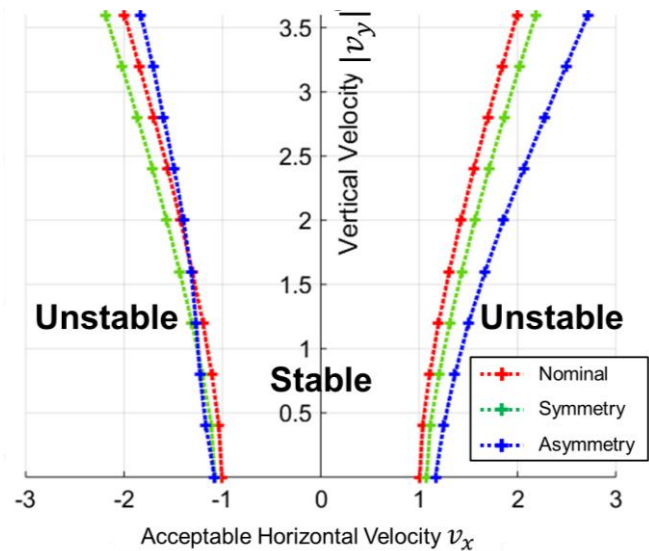


Figure 9 Relationship between vertical velocity and acceptable horizontal velocity

5. Experimental Validation

We conducted landing experiments to verify the results of the simulation. The lander model used in the experiment is shown in Fig. 10. Footpad tilt angle can be changed in 10 degrees increments. The configurations of the footpads and the parameters of the lander model are shown in Table 5 and 6, respectively.

The experimental equipment is shown in Fig. 11. The surface of the floor is filled with No.5 silica sand. The lander model is held by a slider with an electromagnet and moves horizontally by pulling the rope tied to the slider. When the velocity of the lander reaches the setpoint, the electromagnet is turned off by the microcontroller (PSoC5LP) and the lander starts to descend. The motion of the lander during landing is measured by an optical tracking system (OptiTrack). The conditions of the experiment are listed in Table 7. The initial height of the lander is 0.5 m, which is equivalent to 3 m on the Moon. The horizontal velocity v_x ranges from 1 m/s to 2.5 m/s in 0.5 m/s increments. The landings were conducted 3 times for each configuration and velocity.

Table 8 shows the results of the experiment. When v_x is less than 1.5 m/s, overturning did not occur in the all cases. When $v_x = 2.0$ m/s, the nominal configuration overturned 1 out of 3 times, whereas the symmetry configuration overturns 2 out of 3 times. When $v_x = 2.5$ m/s, the nominal and symmetry configuration overturned in the all cases, whereas the asymmetry configuration did not overturn even once.

Figure 12 and 13 show the time history of the body angle and angular velocity during landing, respectively. The horizontal velocity was 2.5 m/s. The nominal



Figure 10 Fabricated lander model.

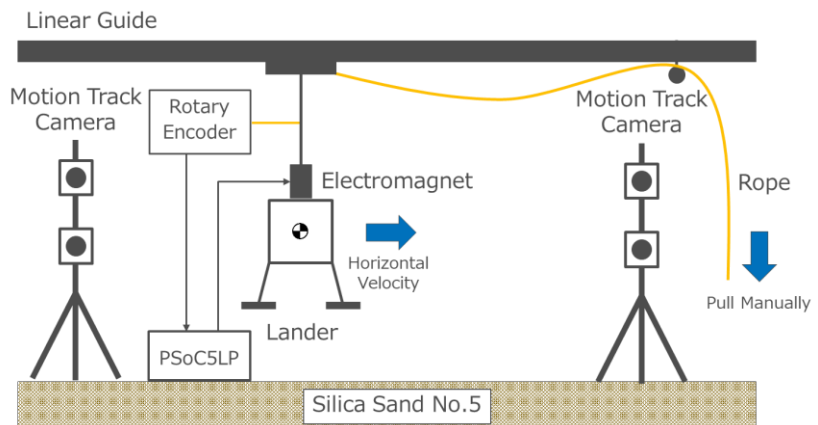


Figure 11 Experimental equipment.

configuration overturned in both the simulation and experiment. In the simulation, both the symmetry and asymmetry configuration did not overturn. However, as

Table 5 The configurations of the footpads

Configuration	Angle β_R	Angle β_F
Nominal	0 deg	0 deg
Symmetry	-20 deg	20 deg
Asymmetry	-60 deg	-20 deg

Table 6 Parameters of the lander model.

Variable	Parameter	Value
m	Mass of lander	2.95 kg
J	Moment of inertia of lander	0.14 kg · m ²
h_b	Height of center of gravity	0.27 m
r_b	Radius of lander	0.15 m
r_p	Width of footpad (z axis)	2 × 80 mm
w_p	Width of footpad (x axis)	80 mm

Table 7 Conditions of the experiment/

Variable	Parameter	Value
g	Gravity acceleration	9.80 m/s ²
ζ	Scaling factor of terrain	2.0
$y(0)$	Initial height of COG	$h_b + 0.5$ m
v_x	Horizontal velocity	1~2.5 m/s
v_y	Vertical velocity	-3 m/s

Table 8 Results of the experiment.

		Nominal			Symmetry			Asymmetry		
		#1	#2	#3	#1	#2	#3	#1	#2	#3
Horizontal Velocity	1.0 m/s	○	○	○	○	○	○	○	○	○
	1.5 m/s	○	○	○	○	○	○	○	○	○
	2.0 m/s	○	○	×	×	○	×	○	○	○
	2.5 m/s	×	×	×	×	×	×	○	○	○

○: Stable x: Overturn

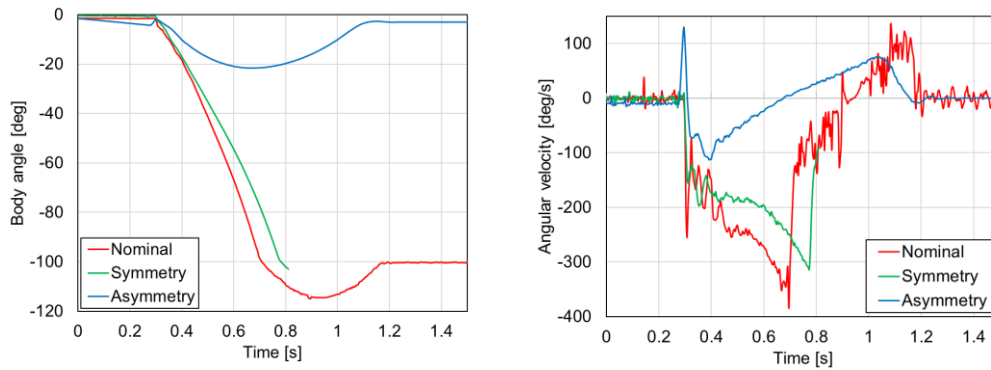


Figure 12 Time history of the body angle and angular velocity (experiment).

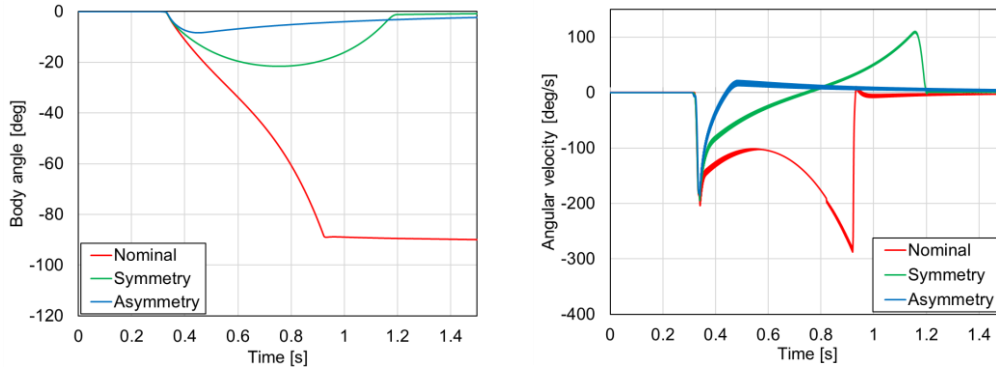


Figure 13 Time history of the body angle and angular velocity (simulation)

for the symmetry configuration, the rear landing gear rose temporarily. In the experiment, the symmetry configuration overturned eventually, though the angular velocity was suppressed. The asymmetry configuration landed without overturning, but the rear landing gear rose temporarily.

The results of the simulation and experiment show that overturning prevention becomes more effective in the order of the asymmetry, symmetry, nominal. Besides, there is a tendency that the overturning prevention effect in the experiment is degraded compared with that in the simulation. This is because the surface of the terrain is deformed by the footpad during landing. In the simulation, the footpad penetrates the soil without deformation.

6. Conclusion

In this study, we proposed a design method of footpad tilt angle for overturning prevention based on RFT and examined the effectiveness of each configuration by simulation and experiment. The results show that the asymmetrically mounted footpads are effective for reducing the risk of overturning if the direction of the horizontal velocity is known.

For future direction, the range of application of the proposed design method should be clarified by precise experimental evaluation. In addition, the design method should be extended to 3D for the actual landing missions.

References

- 1) W.F. Rogers, "Apollo experience report lunar module lander gear subsystem," NASA TN D-6850, June 1972.
- 2) S. Hara, S. Saito, K. Sugita, T. Maeda, "Planetary exploration spacecraft landing gear with three-dimensional linear-rotary-energy-conversion mechanism," *Trans. JSASS Aerospace Tech. Japan*, vol.16, no.7, pp.635-643, Nov. 2018.
- 3) T. Maeda, M. Otsuki, T. Hashimoto, and S. Hara, "Attitude stabilization for lunar and planetary lander with variable damper," *Journal of Guidance, Control, and Dynamics*, pp.1790-1804, Aug. 2016.
- 4) D. Ling, Z. Jiang, W. Cai, S. Zhong, and J. Yang, "Experimental study of sliding forces of lander footpad in simulant lunar soil," *Rock Soil Mechanics*, vol.34, no.7, pp.1847-1853, July 2013.
- 5) M. Sutoh, S. Wakabayashi, and T. Hoshino, "Motion behaviors of landing gear for lunar probes in atmosphere and vacuum tests," *IEEE Robotics and Automation Letters*, vol.2, no.1, pp.313-320, Jan. 2017.
- 6) C. Li, T. Zhang, and D.I. Goldman, "A terradynamics of legged locomotion on granular media," *Science*, vol.339, no.6126, pp.1408-1412, March 2013.
- 7) T. Maeda, M. Otsuki, T. Hashimoto, "Design of Landing-Gear Footpad Based on Resistive Force Generated by Celestial Soil," *Journal of Spacecraft and Rockets*, vol.56, no.1, Jan. - Feb. 2019.
- 8) H. Namikoshi, H. Sugawara, A. Chiba et al., "Preliminary System design of SLIM," 62nd Space Sciences and Technology Conference, 1D03, Kurume, Japan, Oct. 2018.